THE GERONTOLOGICAL SOCIETY OF AMERICA®

Journals of Gerontology: Biological Sciences
cite as: *J Gerontol A Biol Sci Med Sci*, 2021, Vol. 76, No. 4, 601–610
doi:10.1093/gerona/glaa261
Advance Access publication October 14, 2020

OXFORD

Original Article

The Effects of Graded Levels of Calorie Restriction: XVI. Metabolomic Changes in the Cerebellum Indicate Activation of Hypothalamocerebellar Connections Driven by Hunger Responses

Cara L. Green, PhD,[1] Sharon E. Mitchell, PhD,[1] Davina Derous, PhD,[1] Libia A. García-Flores, PhD,[2] Yingchun Wang, PhD,[2] Luonan Chen, PhD,[3] Jing-Dong J. Han, PhD,[4] Daniel E. L. Promislow, PhD,[5] David Lusseau, PhD,[1] Alex Douglas, PhD,[1] and John R. Speakman, PhD[1,2,*]

[1]Institute of Biological and Environmental Sciences, University of Aberdeen, UK. [2]State Key Laboratory of Molecular Developmental Biology, Institute of Genetics and Developmental Biology, Chinese Academy of Sciences, Beijing, China. [3]Key Laboratory of Systems Biology, Innovation Center for Cell Signaling Network, Institute of Biochemistry and Cell Biology, Shanghai Institute of Biological Sciences, Chinese Academy of Sciences, China. [4]Chinese Academy of Sciences Key Laboratory of Computational Biology, Chinese Academy of Sciences-Max Planck Partner Institute for Computational Biology, Shanghai Institutes for Biological Sciences, Chinese Academy of Sciences, China. [5]Department of Pathology and Department of Biology, University of Washington at Seattle.

*Address correspondence to: John R. Speakman, PhD, Institute of Biological and Environmental Sciences, University of Aberdeen, UK. E-mail: j.speakman@abdn.ac.uk

Received: November 12, 2019; Editorial Decision Date: July 28, 2020

Decision Editor: Rozalyn M. Anderson, PhD, FGSA

Abstract

Calorie restriction (CR) remains the most robust intervention to extend life span and improve healthspan. Though the cerebellum is more commonly associated with motor control, it has strong links with the hypothalamus and is thought to be associated with nutritional regulation and adiposity. Using a global mass spectrometry-based metabolomics approach, we identified 756 metabolites that were significantly differentially expressed in the cerebellar region of the brain of C57BL/6J mice, fed graded levels of CR (10, 20, 30, and 40 CR) compared to mice fed ad libitum for 12 hours a day. Pathway enrichment indicated changes in the pathways of adenosine and guanine (which are precursors of DNA production), aromatic amino acids (tyrosine, phenylalanine, and tryptophan) and the sulfur-containing amino acid methionine. We also saw increases in the tricarboxylic acid cycle (TCA) cycle, electron donor, and dopamine and histamine pathways. In particular, changes in L-histidine and homocarnosine correlated positively with the level of CR and food anticipatory activity and negatively with insulin and body temperature. Several metabolic and pathway changes acted against changes seen in age-associated neurodegenerative disorders, including increases in the TCA cycle and reduced L-proline. Carnitine metabolites contributed to discrimination between CR groups, which corroborates previous work in the liver and plasma. These results indicate the conservation of certain aspects of metabolism across tissues with CR. Moreover, this is the first study to indicate CR alters the cerebellar metabolome, and does so in a graded fashion, after only a short period of restriction.

Keywords: Brain, Mass spectrometry, Metabolome, Neurodegeneration, Nutritional regulation

The cerebellum is most commonly associated with motor control (1); however, it is also involved in nutritional regulation and adiposity (2). For example, it plays a role in feeding behavior and, through circadian clock rhythms, has been shown to be centrally involved in the coordination of food anticipatory activity (FAA). We have previously seen that mice under restriction show high levels of FAA for 2 hours pre-feeding, and this behavior was inversely correlated with circulating factors that regulate energy balance such as leptin, insulin,

© The Author(s) 2020. Published by Oxford University Press on behalf of The Gerontological Society of America.
All rights reserved. For permissions, please e-mail: journals.permissions@oup.com.

tumor necrosis factor-α (TNF-α), and insulin-like growth factor-1 (IGF-1) (3). Mice with impaired cerebellar circuitry show no food anticipatory behavior when challenged with calorie restriction (CR) (4). These data suggest an important role for the cerebellum in physiological and behavioral responses to CR. The relationship that exists between the cerebellum and nutritional regulation may be in part due to strong direct connections with the hypothalamus (5), which is a major area of the brain associated with hunger signaling (6).

The hypothalamus controls energy balance through, among other signals, leptin and insulin, which generally circulate in the blood proportionally to body fat content; however, insulin also increases immediately after meals (7). Regulation of energy balance is not only an integration of leptin and insulin signals, but a complex interplay of many tissues and signals. These include adipokines such as adiponectin, interleukin-6, and TNF-α (8) and, peptide hormone signals from the gut such as ghrelin and cholecystokinin, which play a major role in regulating food intake and in body weight maintenance (9). In addition to their prevalence in the hypothalamus, leptin receptors are also highly expressed in the cerebellum (10). These, among other chemical signals, regulate energy balance via food intake and energy expenditure (9). Circulating levels of adipokines (including leptin) (11) and insulin (12) are typically decreased under CR, reflecting the reduced levels of white adipose tissue. These changes are thought to drive improvements in the healthspan and delay the aging process (13,14). Overall, this points to the significance of the cerebellum, as not only associated with somatic motor activity, behavior, and memory through cognitive and sensory functions, but also as a potential coordinator of leptin, nutritional regulation, and adiposity; it is, therefore, an important and crucial region to investigate concerning beneficial CR changes in the brain.

CR improves health parameters in aging individuals and also increases life span. The benefits of CR have been observed across many organisms, from nematodes to primates (15,16). In rodents, CR has been shown to have a linear effect on life span, as calorie intake decreases, life span increases (17). Previously, we found that the brain is relatively protected from mass loss under CR (18). In addition, CR reduces age-related neuronal damage and oxidative stress in the brain (19), potentially through the upregulation of genes associated with neurogenesis and downregulation of inflammatory genes (20). For example, with CR, age-related increases in DNA methylation in cerebellar Purkinje cells are ameliorated, which may indicate that epigenetic changes in cerebellum DNA are driving changes seen in behavior and nutritional regulation (21).

Here we characterize the cerebellum metabolome in male C57BL/6J mice. Owing to the linear relationship between CR and life span in rodents, we applied 4 levels of CR, 10%, 20%, 30%, and 40% (10 CR, 20 CR, 30 CR and 40 CR), for 3 months, with control groups fed 24 hours or 12 hours per day ad libitum (AL). This approach allowed us to identify those metabolites correlated with the extent of restriction and hence likely to be contributing to longevity and reduction of neurodegeneration.

Methodology

Experimental Design

This study consisted of metabolomic data from 49 individual cerebellum samples across 6 different feeding groups, including 4 CR groups and 2 AL-fed groups (Supplementary Material 1). Male mice were randomly allocated to 6 treatment groups: 12 AL (n = 8), 24 AL (n = 8) and 10 (n = 8), 20 (n = 8), 30 (n = 8), and 40 CR (n = 9). The 12 AL group was used as the main control. We initiated CR at 20 weeks; this was done to avoid any effect of CR on development while retaining the effectiveness of increasing life span (22). All mice (except for the 24 AL group) were exposed to the same 12-hour feeding regime during the darkness, and the remaining food was removed at lights on (06:30h). Mice were fed CR (or AL) diets for 12 weeks, before being sacrificed at 32 weeks of age. After death, brains were removed and immediately immersed in isopentane over dry ice, then stored at −80°C. Full details of the overall design and rationale are reported elsewhere (18).

Animals

C57BL/6J male mice were purchased from Charles River (Ormiston, UK). All procedures were reviewed and approved by the University of Aberdeen ethical approval committee and carried out under a Home Office issued license compliant with the Animals (Scientific Procedures) Act 1986. This strain is already known to live longer under CR (23). More information on procedures and measures can be found in the first article of this series (18).

Cerebellum Metabolite Extraction

The cerebellum from individual frozen mouse brain samples was removed and then (≈ 25 mg) homogenized using an ULTRA-TURRAX dispenser T-25 Basic (IKA, Staufen, Germany) at level 5 in 1 mL of chloroform:methanol:water (1:3:1) at 4°C. Samples were agitated for 1 hour at 4°C and centrifuged at 13 000 g for 3 minutes at 4°C. The supernatant was aliquoted into 180 µL samples and stored under argon at −80°C.

Liquid Chromatography–Mass Spectrometry

Samples were analyzed using hydrophilic interaction liquid chromatography (HILIC), which was carried out on a Dionex UltiMate 3000 RSLC system (Thermo Fisher Scientific, Hemel Hempstead, UK) using a ZIC-pHILIC column (150 mm × 4.6 mm, 5 µm column, Merck Sequant). The column was maintained at 30°C and samples were eluted with a linear gradient (20 mM ammonium carbonate in water, A and acetonitrile, B) over 26 minutes at a flow rate of 0.3 mL/min). The injection volume was 10 µL, and samples were maintained at 4°C prior to injection. For the mass spectrometry analysis, a Thermo Orbitrap Exactive (Thermo Fisher Scientific) was operated in polarity switching mode.

Mass Spectrometry Data Processing

To process, extract, and visualize peaks from raw data mzXML files, we used the package *xcms 1.52.0* (24). We extracted mass–charge ratios (m/z), retention times, and intensities for each sample for 2754 peaks in the positive ionization mode and 3155 in the negative ionization mode. We then used the package *MSCombine 1.1* to combine data from the positive and negative ionization modes, which allows us to filter off metabolites identified in both ionization modes (25).

Metabolite Identification

From the combined data set, we identified metabolites from the Human Metabolome Database (HMDB), Kyoto Encyclopedia of Genes and Genomes (KEGG), and LipidMaps databases using the package *xMSannotator 1.3.1* (26). Unknown metabolites were identified using a clustering algorithm that utilizes m/z values, retention times, intensities, and potential adducts and given a confidence score (from 0 to 3). Metabolites with multiple matches were filtered based on the difference between their theoretical and actual monoisotopic mass, the metabolite with the smallest difference was retained, and others were removed. We also filtered based on confidence scored, which are issued by *xMSannotator*; those with a score of 2 or 3 were retained.

Metabolomic Preprocessing

As metabolites, even within samples, show a significant amount of stochastic variation, it is necessary to filter out "noisy" uninformative metabolites. Before metabolomic analysis, a series of processing steps were applied to the entire data set to supply us with the most instructive and stable metabolites for further analysis. Firstly, metabolites were normalized using a log 2 transformation. Second, only metabolites with a signal-to-noise ratio (SNRi = mean/sample standard deviation) ≥15 were kept for analysis (27). Third, metabolites that were missing from 15% or more of all samples were removed.

Statistical Modeling of Differential Metabolite Expression

To detect significantly differentially expressed (SDE) metabolites between treatment groups, an empirical Bayes moderated linear model was fitted to each metabolite (28). The empirical Bayes approach shrinks the estimated sample variances by borrowing information from across metabolites. Comparisons across metabolite fold-changes were made between each level of CR (10, 20, 30, and 40) and 24 AL relative to 12 AL. p values for each comparison were adjusted using the Benjamini–Hochberg procedure using a false-discovery rate of 5% (29). We used the package Devium to produce the orthogonal partial least squares discriminant analysis (OPLS-DA) plots, to complete the validation steps and retrieve metabolite loadings (30). OPLS-DA allows us to discriminate between groups in multivariate data and to determine the most influential metabolites. To validate the OPLS-DA, we carried out 1000 simulations on randomly permuted groups to compare the modeled data to random expectation. We generated a pseudo training set by splitting the data into a testing and training set.

Biological Pathway Analysis

Pathway analysis was conducted in *mummichog* as part of the metabolite identification process and in Ingenuity Pathway Analysis (IPA). For analysis in *mummichog*, metabolites with unadjusted $p \leq .05$ generated by the empirical Bayes linear model for each comparison with 12 AL were used with associated coefficients and retention times. Also, the IPA program allowed us to take advantage of the Ingenuity Knowledge Base, a repository of biological and chemical information from the literature. Metabolite unadjusted p values and coefficients from each comparison relative to 12 AL alongside identifications names (IDs) from either KEGG or HMDB were included.

Correlations With Physiological Parameters

Physical parameters (FAA and insulin levels) were correlated (Pearson's correlation) with metabolite intensities across all mice. Associated p values for each correlation were adjusted using the Benjamini–Hochberg procedure using a false-discovery rate of 5%. FAA was calculated as the number of "activity counts" (by telemetry and data acquisition system) that occurred in the 2 hours prior to lights out. Then it was subtracted this from the total daily activity and called this remainder non-FAA. For more details, please see Ref. (3).

Results

Metabolite Detection and Characterization

We used liquid chromatography–mass spectrometry to detect metabolites in the cerebellum and found that 3155 *m/z* features and 2755 *m/z* features were detected in the negative and positive ionization modes, respectively, which were then combined and filtered. Post-filtering, a total of 3259 *m/z* features were present. Of the filtered metabolites, 756 were SDE in the CR groups when compared to the 12 AL control group ($p \leq .05$), and 167 were SDE at 24 AL relative to 12 AL. Generally, as the level of restriction increased, the number of SDE metabolites also increased, although 10 CR also had a high number of SDE metabolites (Supplementary Material 2). Metabolites were identified using 3 different databases, the HMDB, the KEGG, and LipidMaps. Analysis using the HMDB database revealed 862 unique chemical identifiers, while the use of KEGG produced 2666 unique identifiers and LipidMaps substantially more at 4941. In addition to metabolite IDs yielded from *mummichog* analysis, out of a total of 8469 of these IDs were matched to 841 metabolites (due in part to redundancy between and within databases). A full list of all the SDE metabolites and their fold-changes can be found in Supplementary Material 12 (available at our Open Science Framework https://osf.io/4wfpa/).

Multivariate Analysis

We performed an OPLS-DA on all identified and nonidentified filtered metabolites (n = 3259). The model (Figure 1) indicated that around 50% of the variance (18% in the first 2 components) in the metabolite intensities could be explained by level of CR (single-sample t test between model parameters and permuted parameters $n = 1000$, $p < .001$, RX2 = 50.31, $Q^2 = 0.873$, root mean square error of prediction = 0.611). Loadings from the OPLS-DA model determined metabolites that contributed to the separation of groups. Of

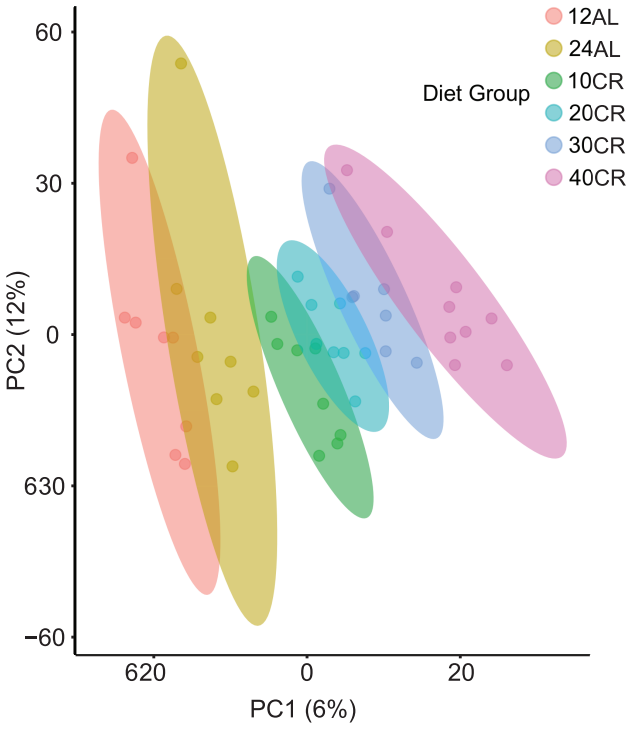

Figure 1. Orthogonal partial least square discriminate analysis (OPLS-DA) demonstrates the differentiation effect of each diet group (12-hour ad libitum fed:12 AL, 24-hour ad libitum fed: 24 AL, 10–40 calorie-restricted: 10 CR, 20 CR, 30 CR, 40 CR) on the filtered and normalized metabolites extracted from the cerebellum, n/group = 7–9. The OPLS-DA plot showed significant separation among samples in the first 2 principal components (PC1 and PC2) based on the model quality parameters: RX2 = 50.31, Q2 = 0.873, and root mean square error of prediction = 0.611.

3259 *m/z* features, 466 features (or ≈14% of all metabolites) were judged to be significantly contributing to discrimination between treatment groups, using a false-discovery rate cutoff $p < .05$. Of these, we were able to identify 126 (Supplementary Material 3). Our OPLS-DA model indicated changes in several different groups of metabolites. These included metabolites involved in DNA and RNA syntheses such as adenosine and thymine, changes in carnitines, for example, *O*-butanoylcarnitine and dodecanoylcarnitine and amino acids, L-lysine, L-histidine, L-valine and L-proline and metabolites involved in energy production from carbohydrates, guanosine diphosphate mannose, *N*-Acetyl-L-citrulline, and 4-fumaryl-acetoacetate.

Pathway Enrichment Analysis

To determine pathways that change between the 12 AL group and each of the CR groups, we performed pathway enrichment analyses in both *mummichog* (Supplementary Material 4) and IPA (Supplementary Material 5). For *mummichog* analysis, all filtered *m/z* values were entered ($n = 3259$), with associated *p* values, fold-changes relative to 12 AL, and retention times (Figure 2). Only metabolites with KEGG or HMDB IDs ($n = 376$) were included in the IPA analysis with their corresponding *p* values and log fold-changes relative to 12 AL. The level of CR has been shown to have a positive linear relationship with life span (14,31). To this end, we correlated metabolites with the level of restriction to determine metabolites that are most likely associated with both nutritional regulation and potential changes in life span (Table 1, A). The correlation coefficients from this analysis were entered into *mummichog*, along with their corresponding *m/z* values, to find pathways that were potentially associated with longevity in the cerebellum (Table 2).

Regarding DNA components results, we found significant differences with CR, including significant decreases of guanosine and thymine at 40 CR (Supplementary Material 6) and increase of adenosine at all CR levels (Supplementary Material 4). At the pathway level, there were increases in several components at all CR levels involving processes that included nucleotides, nucleosides, and ribonucleotides, and these consisted of guanosine and adenosine nucleotide degradation, purine nucleotide and ribonucleoside degradation, and purine de novo biosynthesis. Also, adenosine monophosphate correlated significantly positively with level of CR (adjusted $p = .016$, $R = 0.555$; Table 1, A), as did metabolites in the tRNA charging pathway ($p = .004$) indicating their association with responses to nutrition (Table 2).

Many metabolites that are not directly synthesized in the brain must be transferred across the blood–brain barrier, which has a transporter responsible for the uptake of the large neutral amino acids (principally tyrosine, tryptophan, leucine, isoleucine, valine, and methionine) (32). We found that many amino acids significantly changed with CR in several different pathways (Supplementary Material 7). In addition, according to *mummichog* pathway enrichment, components of the tyrosine degradation pathway appeared significantly increased at all levels of CR relative to 12 AL but not at 24 AL, where the pathway was not significant. Also, the pathways of other aromatic amino acids, phenylalanine and tryptophan, were increased at 10 CR (Supplementary Material 5). In particular, components associated with methionine pathways

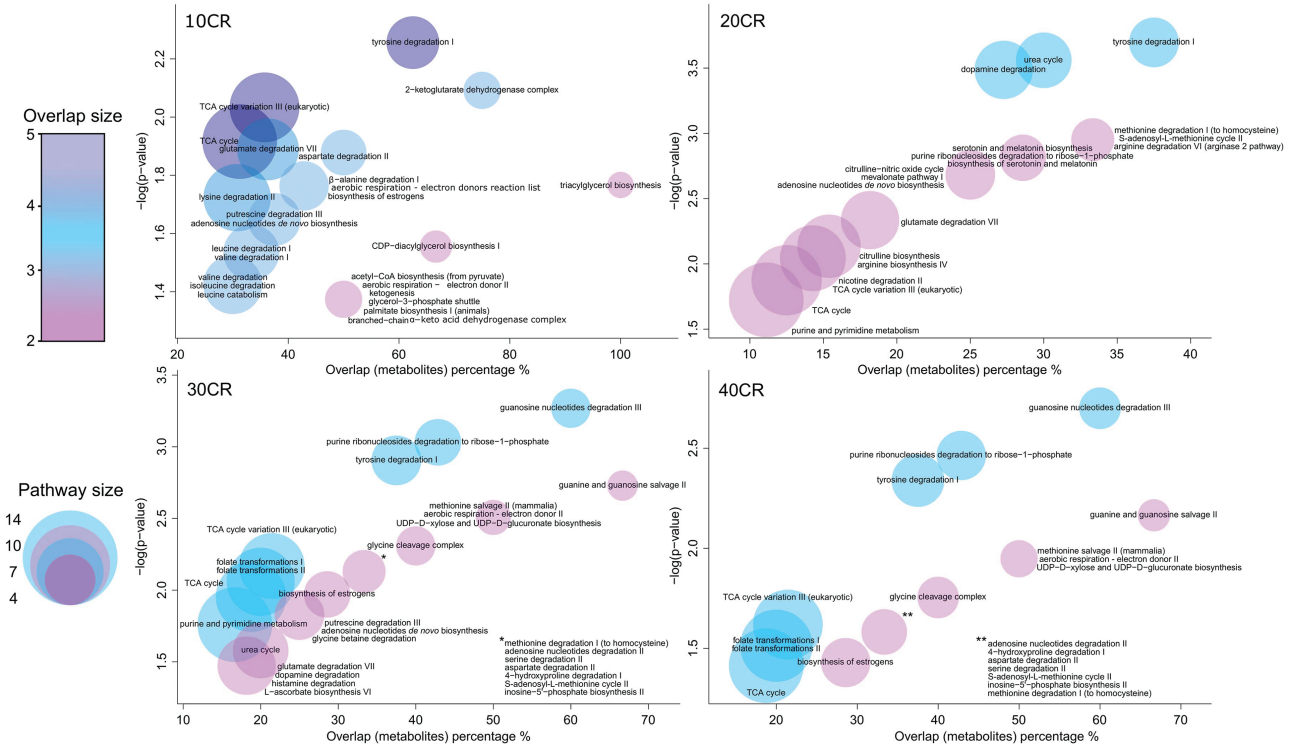

Figure 2. Visualization of pathway changes at 4 levels of calorie restriction (10–40 CR) relative to the 12-hour ad libitum fed (12 AL) group. The number of significantly differentially expressed metabolites identified in our analysis relative to the total number of metabolites in the pathway expressed as a percentage is shown on the x-axis. Pathway significance is expressed as –log(*p* value) on the y-axis. Number of significant metabolites identified in our analysis in each pathway is expressed as overlap size in the color chart. Total number of metabolites in the pathway expressed by circle size. Significantly altered pathways ways (*p* value adjusted for permutations $p < .05$) as reported from *mummichog*, which uses BioCyc pathway database.

Table 1. Metabolite Intensities for Each Individual Mouse Were Correlated (Pearson's correlation) With Level of CR (A), Insulin (B), and TNF-α (C) for Each Mouse ($n = 45$)

	Metabolite	*R*	*p* Value
A	Homocarnosine	0.801	.025
	L-Histidine	0.698	.039
	Ethyl glucuronide	0.656	.034
	Xanthopterin-B2	0.641	.006
	12-di-(9Z-hexadecenoyl)-sn-glycero-3-phosphate	0.607	.022
	8-aminocaprylic acid	0.566	.006
	AMP	0.555	.016
	D-alanyl-D-alanine	0.509	.034
	L-Octanoylcarnitine	0.494	.008
	L-2-Amino-4-(hydroxymethylphosphinyl) butanoate	0.378	.012
	Trans-2-Dodecenoylcarnitine	0.288	.032
	Sulfometuron	−0.344	.041
	Flavonol 3-O-beta-D-glucosyl-(1–2)-beta-D-glucoside	−0.474	.037
	Paracetamol sulfate	−0.492	.021
	L-arginino-succinate	−0.503	.025
	Homovanillate	−0.547	.041
	Selenocystine	−0.566	.016
	Epi-Tulipinolide diepoxide	−0.585	.021
	4-fumaryl-acetoacetate	−0.618	.006
	Echothiophate	−0.64	.004
	3-Hydroxy-89-methylenedioxycoumestan	−0.665	.003
	Laudanosine	−0.665	.041
	L-valine	−0.704	.009
	4-acetamidobutanal	−0.815	.012
B	(3S5S)-Carbapenam-3-carboxylic acid	0.761	.027
	Paracetamol sulfate	0.674	.041
	4-Fumaryl-acetoacetate acid	0.618	.006
	3-Hydroxy-89-methylenedioxycoumestan	0.561	.019
	Selenocystine	0.556	.037
	UDP-D-xylose	0.523	.047
	Guazatine	0.514	.046
	13-dihexadecanoyl-2-hydroxy-glycerol (d5)	0.467	.027
	4-(3-pyridyl)-3-butenoate	0.46	.046
	L-proline	0.446	.019
	Triethanolamine	0.301	.041
	AMP	−0.376	.039
	Trans-2-Dodecenoylcarnitine	−0.386	.027
	D-Glutamic acid	−0.399	.047
	N-Nitrosoguvacoline	−0.497	.027
	Ethyl glucuronide	−0.504	.041
	L-Histidine	−0.536	.027
	8-aminocaprylic acid	−0.608	.027
	Homocarnosine	−0.665	.031
C	7-Deoxyloganetin	0.816	.041
	3-Methylhistidine	0.541	.003
	Phthalocyanine	0.527	.01
	Formothion	0.394	.01
	5-Methylcytidine	0.376	.027
	Glycerophosphoethanolamine	0.371	.044
	11-Deoxytetrodotoxin	0.319	<.001
	N-octadecanoyl-tyrosine	−0.429	.01
	Dodecanoylcarnitine	−0.486	.036
	Coenzyme A	−0.499	.011

Notes: AMP = adenosine monophosphate; CR = calorie restriction; TNF-α = tumor necrosis factor-α. Benjamini–Hochberg (BH) adjusted *p* values used to control for a false-discovery rate of 5%. Metabolites are sorted by their *R*-value significance.

also appeared to increase across all levels of CR, frequently appearing in both the *mummichog* and IPA analyses (Supplementary Material 4 and 5). Except for 10 CR, where the components of the *S*-adenosyl-L-methionine pathway were significantly increased in the CR treatment groups (Supplementary Material 4). Although most pathways were increased or unchanged with CR, at 10 CR, components of both lysine and valine pathways were decreased in both IPA and *mummichog*. Most amino acid pathways at 24 AL showed a decrease relative to 12 AL, including methionine, phenylalanine, and lysine pathways; however, arginine biosynthesis was increased (in IPA). Correlation of metabolites revealed some amino acids and associated molecules that had a linear relationship with CR, L-histidine, homocarnosine, and D-alanyl-D-alanine correlated positively with the level of CR, whereas L-arginino-succinate, selenocystine, L-valine, and 4-acetamidobutanal (involved in arginine and proline metabolism) correlated negatively (Table 1, A; Supplementary Material 8).

Amino acids form the precursors for neurotransmitters in the brain, and these include tryptophan, tyrosine, and phenylalanine, which act as precursors for serotonin, dopamine, and norepinephrine, respectively (33). We saw increases in the dopamine signaling pathway at all levels of CR and at 24 AL relative to 12 AL, though not all metabolites were significant at all levels (Supplementary Material 9). Additionally, using IPA pathway analysis, at 20 CR and 30 CR, we saw an increase in components of the levodopa pathway, and at 20 CR, we saw an increase in serotonin and melatonin biosynthesis. According to *mummichog*, components of the biosynthesis of estrogens pathway changed at 40 CR, but the pathways at 30 CR overall remained unchanged, whereas at 10 CR components increased overall. At 24 AL components of several catecholamine and steroid pathways were increased, including biosynthesis of corticosteroids, dopamine degradation, biosynthesis of estrogens by *mummichog* pathway, on the other hand, catecholamine biosynthesis and noradrenaline and adrenaline degradation showed significant changes by IPA pathway analysis. Moreover, the correlation of metabolites with the level of CR indicated that the major catecholamine metabolite homovanillate has an inverse relationship with increasing restriction (Table 1, A; Supplementary Material 8).

Amino acids, primarily from muscle proteolysis, also act as substrates for energy during starvation, when hepatic gluconeogenesis is crucial in providing glucose for the brain during starvation. Pathway enrichment indicated that there are changes in groups of metabolites associated with the production of energy through the oxidation of carbohydrates and proteins. The tricarboxylic acid cycle (TCA) cycle and electron donor pathways were increased at all CR levels relative to 12 AL, although not all metabolites from these pathways reached significance at all levels (Supplementary Material 10). In addition to these, components of the acetyl-CoA biosynthesis pathway were also increased at 10, 20, and 30 CR. At 10 CR, there were several other

Table 2. Pathways That Change Based on Filtered, Normalized Metabolites That Have a Linear Relationship (Pearson's Correlation) With Level of Restriction That May Be Associated With Longevity in the Cerebellum

Pathway	Overlap Size	Pathway Size	*p* Value	Positive Association
tRNA charging pathway	3	19	.004	2/3
Citrulline-nitric oxide cycle	2	8	.006	1/2
Glycolysis V (Pyrococcus)	2	9	.007	1/2
Glycolysis I	2	10	.008	1/2
Urea cycle	2	10	.008	1/2
Arginine biosynthesis IV	2	13	.011	1/2
Gluconeogenesis I	2	14	.012	1/2

Notes: Significantly altered pathways (*p* value adjusted for permutations $p < .05$) as reported from mummichog, which uses BioCyc pathway database. Positive association is the number of significantly upregulated metabolites/total number of significant metabolites found in our sample in the pathway. Metabolites are sorted by their *p* value significance.

pathways increased, including ketogenesis and ketolysis, in addition to ethanol degradation and gluconeogenesis (Supplementary Material 11). This result is surprising as ketogenesis acts in opposition to both ketolysis and gluconeogenesis; however, it may indicate a transition period during lower levels of CR, where metabolic substrate changes are in flux (34). Furthermore, one should also take into consideration that the ketogenesis pathway has 2/8 metabolites upregulated, and ketolysis has 2/9 metabolites upregulated (Supplementary Material 5). This result highlights the poor "hit rate" of metabolites per pathway, which is a limitation of current metabolomics analyses. This is due to the imprecise nature of metabolite identification in global metabolomics and the structure of metabolic pathways. Often, pathways with very similar metabolites will both appear as significantly altered, even if they are opposing. Thus, new bioinformatics tools are necessary to improve the metabolite/pathway databases that are required to get more accurate and global insights into the metabolome. Gluconeogenesis was also increased at 24 AL, in addition to glycolysis, glucose degradation, whereas ethanol degradation and NAD biosynthesis were decreased. Correlation of metabolites with the level of CR yielded correlation coefficients that were entered into *mummichog* in an attempt to define pathways that may be associated with modulation of behavior in the brain upon nutritional deficit. Pathways containing metabolites with significant associations with the level of CR were mainly related to the production of energy, glycolysis, gluconeogenesis, and the citrulline–nitric oxide cycle (Table 2).

Correlations With Physical, Hormonal, and Transcriptomic Measures

This metabolomics cerebellum study is part of a series of articles that aim to understand CR effects compared to AL affects from different perspectives in the same mice (C57BL/6J strain). Here we tested for correlations between several physiological variables that have been analyzed in previous articles: PA (3), FAA (3), and body temperature (35). FAA correlated positively with L-octanoylcarnitine ($R = 0.485$, $p = .029$) and negatively with selenocystine ($R = -0.556$, $p = .044$). We also correlated metabolites with circulating hormonal measures that have shown a relationship with the hypothalamus, the control energy balance, and have shown a role in the aging process (36). L-histidine, homocarnosine, and trans-2-dodecenoylcarnitine correlated negatively with insulin levels ($R = -0.536$, $p = .027$, $R = -0.665$, $p = .031$, and $R = -0.386$, $p = .027$, respectively; Table 1, B; Supplementary Material 8). In addition, 4-fumarylacetoacetic acid (an intermediate of tyrosine metabolism), L-proline, L-argino-succinate, selenocystine, triethanolamine, and UDP-D-xylose were significantly positively correlated with insulin. Conversely, adenosine monophosphate, ethyl glucuronide, and D-glutamic acid were correlated negatively with insulin. Several metabolites correlated positively with TNF-α (Table 1, C; Supplementary Material 8), including 3-methylhistidine and negatively, such as coenzyme A and dodecanoylcarnitine. We correlated cerebellar histidine and homocarnosine metabolites with hypothalamic mRNA levels of the histamine receptors (Hrh1, Hrh2, and Hrh3) (6), to determine whether there was a possible hypothalamocerebellar relationship, but we did not find a correlation. Although we did find that L-histidine and homocarnosine (a dipeptide formed of histamine and gamma aminobutyric acid [GABA]) showed a significant correlation ($R = 0.984$, $p < .001$). Furthermore, hunger signaling responses in the hypothalamus (6) are also driven by FAA, PA, insulin, and leptin, and the correlation of these measures with L-histidine and homocarnosine indicated several significant relationships. Homocarnosine and L-histidine correlated significantly positively with FAA and negatively with average daily body temperature (Figure 3).

Discussion

We used graded levels of CR to detect changes in the metabolome, which due to the linear relationship between the level of CR and life span, may be associated with longevity. Previous transcriptomic analysis in the same mice showed that changes in hunger signaling pathways in the hypothalamus might be significant in conferring the beneficial effect of CR (6). Given the functional connections between the cerebellum and hypothalamus, we would expect that changes in the cerebellar metabolome would potentially be crucial in modulating the beneficial effects of CR. As the cerebellum plays a role in motor coordination, we might also expect metabolomic changes to be associated with behavioral changes such as increased FAA that is observed with increasing CR.

The cerebellum is a key brain region involved in coordination, precision, timing, and motor skills and is thought to have strong bilateral connections with the hypothalamus (5). Histaminergic fibers are also considered an essential component of the hypothalamocerebellar circuit. Histaminergic fibers are thought to be critical in integrating autonomic and somatic centers and they play a role in modulating activities in the age-related cerebellar circuitry (37,38). There is a growing body of evidence to suggest that histamine is one of the key neuromodulators of cerebellum activity and is central to the histaminergic system (39,40). Histidine is known to readily enter the brain from the blood, and an increase in brain levels of histidine and homocarnosine has been seen previously in protein-deficient rats (41). Decreased histaminergic activity may also contribute to a reduction in GABAergic neurons, which can, directly and indirectly, affect cognition and memory through the hippocampus (42). We found that both L-histidine, the precursor of histamine, and homocarnosine, a brain-specific dipeptide composed of histamine and GABA, were significantly positively associated with the level of CR (Table 1, A); this may indicate that some neurotransmitter changes in the brain may change relative to the amount of

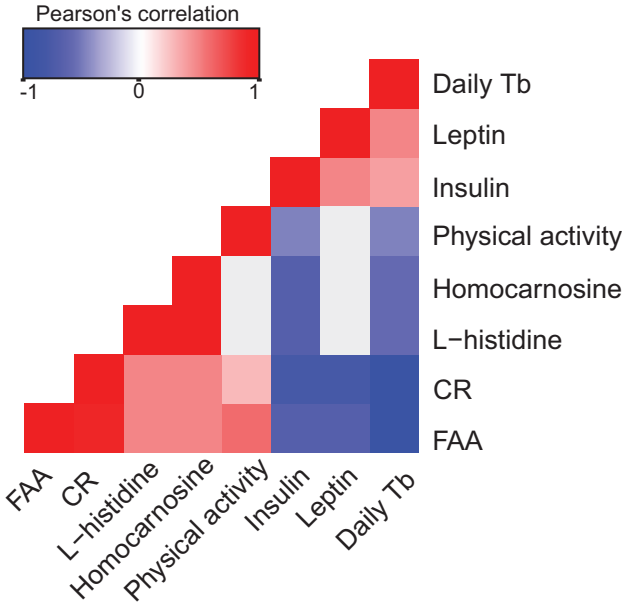

Figure 3. Pearson's correlations between metabolites associated with L-histamine and hormone and behavioral responses associated with hunger signaling across individual mice from all treatment groups ($n = 45$). Pearson's correlations were adjusted using Benjamini–Hochberg procedure for false discovery, $p \leq .05$. Red = significant positive correlation, blue = significant negative correlation, and gray = nonsignificant.

restriction. In addition, these metabolites are strong antioxidants that are found in the muscle and brain, where oxidation rates are highest (43). This result suggests that CR may be an important promoter of these neurotransmitters in the cerebellum tissue, which in turn may indicate that CR can diminish age-associated disorders, including neurodegeneration, through upregulation of these molecules. In addition, hypothalamocerebellar coordination has been shown to promote motor skills in rats through histamine and its receptors. This occurs via excitation of the cerebellar neurons through activation of Hrh2 receptors in hypothalamic histaminergic projections in the cerebellar fastigial nucleus, which has been shown to promote motor performance in rats (44). While it has been shown that mRNA levels of histamine receptors, Hrh1, Hrh2, and Hrh3, are decreased in most regions of C57BL/6 mouse brains with age (37), our hypothalamic transcriptomic analysis did not show any significant changes with CR (6). However, from this previous study of hypothalamus transcription, which was completed on the same mice, we did not find a relationship between levels of L-histidine or homocarnosine and levels of histamine receptors in the hypothalamus, despite the strong hypothalamocerebellar connections that exist.

Our findings suggest that an increase in the level of CR can affect critical processes related to DNA in the cerebellum, as we saw increases in nucleotide and nucleoside pathways and nucleobases at all CR levels (Supplementary Material 4–6). It has been reported that nucleotide biosynthetic pathways, and also precursor pathways, are catalyzed by several enzymes, the genes of which are regulated by the transcription factor MYC (45), which we found was significantly activated at 40 CR in the hypothalamus in our previous analysis of these mice (6). This finding supports what we see metabolically and may suggest direct activation of metabolic changes, such as increased cell proliferation and energy metabolism in the cerebellum, as coordinated through the hypothalamus during CR. Nucleotides such as cytosine, adenosine, and guanine are the building blocks of DNA and are also involved in many metabolic processes (46). Notably, an increase in nucleotide synthesis is required during cell proliferation for DNA replication and repair. This concurs with previous research indicating that unscheduled DNA repair declines with age in AL-fed rats and that unscheduled DNA repair is significantly increased in the liver and kidney of Fischer rats under CR and is associated with increased longevity (47). Furthermore, 40 CR has been found to improve DNA repair in skin cells of both rats and mice (48). In neurons, however, the situation may be different, and it is thought that although neurons have high metabolic activity, they generally have a low level of basal DNA repair, and this may leave them more susceptible to oxidative damage as most cells in the brain exist in a post-mitotic state. Nevertheless, with CR initiated from 6 to 28 months (when sacrificed) in rats, alkaline DNase activity improved in the cerebellum, brain-cerebral cortex, corpus striatum, hippocampus, and pituitary, and overall maintenance of DNA repair via DNases and DNA polymerases in the brains of rats appeared improved with CR (49).

The production of nucleotides requires several resources, including sources of carbon, nitrogen, and energy (46). We saw increases in changes in amino acid pathways (Supplementary Material 4–7) and the TCA cycle (Supplementary Material 4 and 5), which may indicate the potential provision of these resources. In addition, L-proline, a neuroexcitatory amino acid, was negatively correlated with CR in the cerebellum in this study. L-proline in these mice was also significantly positively correlated with circulating insulin levels (36) (Table 1, B). Previously, IGF-1 has been shown to stimulate the uptake of L-proline (50), and we found that IGF-1 was reduced with CR (36). However, it may be that the reduced levels of circulating insulin and IGF-1 with increasing CR result in reduced L-proline uptake in neuronal cells, and by proxy, reduce neuronal damage. Thus, our results may suggest that CR may be a potentially noninvasive method to reduce neurodegeneration and associated disorders in a linear fashion.

Additionally, several carnitine metabolites, which are involved in transporting fatty acids across the mitochondrial membrane for β-oxidation (51), were found to be significantly increased in one or more CR groups (Table 1, A). Several carnitines were shown to discriminate between treatment groups; in particular, L-octanoylcarnitine and trans-2-dodecenoylcarnitine were positively associated with CR and trans-2-dodecenoylcarnitine was negatively correlated with insulin (Table 1, B), which may indicate activation of cerebellar pathways through hormonal changes associated with CR. Furthermore, in previous studies with the same mice, carnitines metabolites increased both in the liver (52) and in the plasma (53), and they showed positive correlations with the level of CR and highlighting their significance in multiple tissues and potential relevance to longevity.

It should be noted that in murine and human brain tissue, aging is associated with an increase in inflammation and oxidative stress, which may establish themselves fairly early in life (54,55). It has been shown that CR can reduce age-related neuronal damage and oxidative stress in the brain (19,56). However, in our mice, there was no indication that CR affected common measures of oxidative stress, and the antioxidant activity was actually lowered with CR (36); however, plasma metabolomics did show increases in several, potentially antioxidant, vitamin E metabolites (53). Although we could not measure hypothalamic reactive oxygen species levels due to lack of tissue, RNAseq analysis showed an increase in the expression of the neuropeptides Neuropeptide Y and Agouti-related protein with

CR (6). Together with the reduction of the leptin levels (3), this could suggest improved leptin sensitivity, in addition to a reduction of the levels of reactive oxygen species in the brain. On the other hand, CR reduces the levels of oxidative protein damage in mice (57) and rats (58), and age-related loss of motor coordination is correlated with oxidative molecular damage within the cerebellum (59). In previous work, we found that circulating TNF-α was reduced with CR (36), and transcriptomic analysis indicated that the transcription factor nuclear factor-kappa B was inhibited at all CR levels (6), which reflects a reduced state of inflammation. Increased protein turnover and DNA repair, indicated by the cerebellar metabolomics, further suggest that CR can reduce damage through inflammation. The increase in adenosine and guanine that we see in nucleotide pathways (Supplementary Material 4 and 5) may support increased levels of RNA production, which would result in increased protein synthesis. Protein translation is also indicative of higher cell turnover, repair and maintenance, and, therefore, lower damage and reduced neurodegeneration (60).

Particularly apparent in our study were the increases in the aromatic amino acid pathways, tyrosine, phenylalanine, and tryptophan. L-tyrosine and L-tryptophan produce dopamine and serotonin in the brain (33). We found that at 20, 30, and 40 CR, dopamine pathways were increased (Supplementary Material 4, 5, and 9). In addition, we showed in these same mice that dopaminergic mechanisms in the brain are associated with the motivational aspects of eating, and in the hypothalamus *Drd5* (dopamine receptor) correlated significantly positively with the level of CR, indicating that as mice became increasingly restricted, the level of this dopamine receptor in the hypothalamus increased (6). These discoveries, taken together, may suggest that cerebellar metabolism can be modulated through nutritional changes detected by the hypothalamus through hypothalamocerebellar connections. Interestingly, the dopamine pathway was also increased in the 24 AL group, which may also be activated through disrupted circadian rhythms from having constant access to food, changes which we saw in our previous study in the hypothalamus (6,61,62).

In conclusion, our study indicated several changes in cerebellum metabolic pathways associated with CR, involving neurotransmitters, amino acids, and nucleobases. Together these changes suggest that in addition to the protection of brain mass with CR (18), reduction in insulin and proline may reduce levels of neuronal damage. These signals may be occurring directly in the cerebellum via neurotransmitters such as histamine (via increases in pathway intermediates L-histidine and homocarnosine), but also through afferent links with the hypothalamus. Increasing DNA and protein turnover may additionally act to reduce oxidative damage in cerebellar neurons. Reducing such damage is integral to delaying neurodegenerative disorders such as Alzheimer's and Parkinson's disease (63–65).

Supplementary Material

Supplementary data are available at *The Journals of Gerontology, Series A: Biological Sciences and Medical Sciences* online.

Funding

The work was supported by the UK Biotechnology and Biological Sciences Research Council BBSRC (BB/G009953/1, BB/P009875/1, and BB/J020028/1 to J.R.S.), the National Science Foundation of China (91649108), and the KC Wong Education Foundation also to J.R.S. A studentship supported C.L.G. from the BBSRC EastBio Doctoral Training Partnership (1438803). C.L.G. received support from the laboratory of D.E.L.P. D.E.L.P was supported in part by the National Institutes of Health grant AGO49494.

Acknowledgments

We are grateful to the animal care staff at the University of Aberdeen.

Conflict of Interest

None declared.

Data Availability

Supplementary Material for this article and others in the Graded Calorie Restriction series can be found at our Open Science Framework (https://osf.io/4wfpa/).

References

1. Baumann O, Borra RJ, Bower JM, et al. Consensus paper: the role of the cerebellum in perceptual processes. *Cerebellum*. 2015;14:197–220. doi:10.1007/s12311-014-0627-7
2. Mahler P, Guastavino JM, Jacquart G, Strazielle C. An unexpected role of the cerebellum: involvement in nutritional organization. *Physiol Behav*. 1993;54:1063–1067. doi:10.1016/0031-9384(93)90325-a
3. Mitchell SE, Delville C, Konstantopedos P, et al. The effects of graded levels of calorie restriction: V. Impact of short term calorie and protein restriction on physical activity in the C57BL/6 mouse. *Oncotarget*. 2016;7(15):19147–19170. doi:10.18632/oncotarget.8158
4. Mendoza J, Pévet P, Felder-Schmittbuhl MP, Bailly Y, Challet E. The cerebellum harbors a circadian oscillator involved in food anticipation. *J Neurosci*. 2010;30:1894–1904. doi:10.1523/JNEUROSCI.5855-09.2010
5. Onat F, Cavdar S. Cerebellar connections: hypothalamus. *Cerebellum*. 2003;2:263–269. doi:10.1080/14734220310016187
6. Derous D, Mitchell SE, Green CL, et al. The effects of graded levels of calorie restriction: VI. Impact of short-term graded calorie restriction on transcriptomic responses of the hypothalamic hunger and circadian signaling pathways. *Aging (Albany NY)*. 2016;8(4):642–661. doi:10.18632/aging.100895
7. Morton GJ. Hypothalamic leptin regulation of energy homeostasis and glucose metabolism. *J Physiol*. 2007;583(Pt 2):437–443. doi:10.1113/jphysiol.2007.135590
8. Ahima RS, Lazar MA. Adipokines and the peripheral and neural control of energy balance. *Mol Endocrinol*. 2008;22:1023–1031. doi:10.1210/me.2007-0529
9. Lean ME, Malkova D. Altered gut and adipose tissue hormones in overweight and obese individuals: cause or consequence? *Int J Obes (Lond)*. 2016;40:622–632. doi:10.1038/ijo.2015.220
10. Savioz A, Charnay Y, Huguenin C, Graviou C, Greggio B, Bouras C. Expression of leptin receptor mRNA (long form splice variant) in the human cerebellum. *Neuroreport*. 1997;8:3123–3126. doi:10.1097/00001756-199709290-00023
11. Fernández-Galaz C, Fernández-Agulló T, Pérez C, et al. Long-term food restriction prevents ageing-associated central leptin resistance in Wistar rats. *Diabetologia*. 2002;45(7):997–1003. doi:10.1007/s00125-002-0851-4
12. Barzilai N, Banerjee S, Hawkins M, Chen W, Rossetti L. Hepatic Glucose Metabolism In Aging caloric restriction reverses hepatic insulin resistance in aging rats by decreasing visceral fat. *J Clin Invest*. 1998;101(7):1353–1361. Accessed July 25, 2017. http://www.jci.org
13. Weindruch R, Walford RL, Fligiel S, Guthrie D. The retardation of aging in mice by dietary restriction: longevity, cancer, immunity and lifetime energy intake. *J Nutr*. 1986;116:641–654. doi:10.1093/jn/116.4.641
14. Merry BJ. Molecular mechanisms linking calorie restriction and longevity. *Int J Biochem Cell Biol*. 2002;34:1340–1354. doi:10.1016/s1357-2725(02)00038-9

15. Fontana L, Partridge L, Longo VD. Extending healthy life span-from yeast to humans. *Science*. 2010;328(5976):321–326. doi:10.1126/science.1172539
16. Mattison JA, Colman RJ, Beasley TM, et al. Caloric restriction improves health and survival of rhesus monkeys. *Nat Commun*. 2017;8:14063. doi:10.1038/ncomms14063
17. Derous D, Mitchell SE, Green CL, et al. The effects of graded levels of calorie restriction: VII. Topological rearrangement of hypothalamic aging networks. *Aging (Albany NY)*. 2016;8:917–932. doi:10.18632/aging.100944
18. Mitchell SE, Tang Z, Kerbois C, et al. The effects of graded levels of calorie restriction: I. Impact of short term calorie and protein restriction on body composition in the C57BL/6 mouse. *Oncotarget*. 2015;6(18):15902–15930. doi:10.18632/oncotarget.4003
19. Gillette-Guyonnet S, Vellas B. Caloric restriction and brain function. *Curr Opin Clin Nutr Metab Care*. 2008;11:686–692. doi:10.1097/MCO.0b013e328313968f
20. Wu P, Shen Q, Dong S, Xu Z, Tsien JZ, Hu Y. Calorie restriction ameliorates neurodegenerative phenotypes in forebrain-specific presenilin-1 and presenilin-2 double knockout mice. *Neurobiol Aging*. 2008;29:1502–1511. doi:10.1016/j.neurobiolaging.2007.03.028
21. Lardenoije R, van den Hove DLA, Vaessen TSJ, et al. Epigenetic modifications in mouse cerebellar Purkinje cells: effects of aging, caloric restriction, and overexpression of superoxide dismutase 1 on 5-methylcytosine and 5-hydroxymethylcytosine. *Neurobiol Aging*. 2015;36:3079–3089. doi:10.1016/j.neurobiolaging.2015.08.001. http://www.sciencedirect.com/science/article/pii/S0197458015004121?via%3Dihub
22. Yu BP, Masoro EJ, McMahan CA. Nutritional influences on aging of Fischer 344 rats: I. Physical, metabolic, and longevity characteristics. *J Gerontol*. 1985;40:657–670. doi:10.1093/geronj/40.6.657
23. Swindell WR. Dietary restriction in rats and mice: a meta-analysis and review of the evidence for genotype-dependent effects on lifespan. *Ageing Res Rev*. 2012;11:254–270. doi:10.1016/j.arr.2011.12.006
24. Smith CA, Want EJ, O'Maille G, Abagyan R, Siuzdak G. XCMS: processing mass spectrometry data for metabolite profiling using nonlinear peak alignment, matching, and identification. *Anal Chem*. 2006;78:779–787. doi:10.1021/ac051437y
25. Calderón-Santiago M, Fernández-Peralbo MA, Priego-Capote F, Luque de Castro MD. MSCombine: a tool for merging untargeted metabolomic data from high-resolution mass spectrometry in the positive and negative ionization modes. *Metabolomics*. 2016;12(3):43. doi:10.1007/s11306-016-0970-4
26. Uppal K, Walker DI, Jones DP. xMSannotator: An R package for network-based annotation of high-resolution metabolomics data. *Anal Chem*. 2017;89:1063–1067. doi:10.1021/acs.analchem.6b01214
27. Hoffman JM, Soltow QA, Li S, Sidik A, Jones DP, Promislow DE. Effects of age, sex, and genotype on high-sensitivity metabolomic profiles in the fruit fly, *Drosophila melanogaster*. *Aging Cell*. 2014;13:596–604. doi:10.1111/acel.12215
28. Smyth GK. Linear models and empirical Bayes methods for assessing differential expression in microarray experiments. *Stat Appl Genet Mol Biol*. 2004;3:Article3. doi:10.2202/1544-6115.1027
29. Benjamini Y, Hochberg Y. Controlling the false discovery rate: a practical and powerful approach to multiple testing. *J R Stat Soc B*. 1995;57(1):289–300. doi:10.2307/2346101
30. Wanichthanarak K, Fahrmann JF, Grapov D. Genomic, proteomic, and metabolomic data integration strategies. *Biomark Insights*. 2015;10(suppl 4):1–6. doi:10.4137/BMI.S29511
31. Speakman JR, Mitchell SE, Mazidi M. Calories or protein? The effect of dietary restriction on lifespan in rodents is explained by calories alone. *Exp Gerontol*. 2016;86:28–38. doi:10.1016/j.exger.2016.03.011
32. Pardridge WM. Brain metabolism: a perspective from the blood-brain barrier. *Physiol Rev*. 1983;63:1481–1535. doi:10.1152/physrev.1983.63.4.1481
33. Fernstrom JD. Effects on the diet on brain neurotransmitters. *Metabolism*. 1977;26:207–223. doi:10.1016/0026-0495(77)90057-9
34. Bruss MD, Khambatta CF, Ruby MA, Aggarwal I, Hellerstein MK. Calorie restriction increases fatty acid synthesis and whole body fat oxidation rates. *Am J Physiol Endocrinol Metab*. 2010;298:E108–E116. doi:10.1152/ajpendo.00524.2009
35. Mitchell SE, Delville C, Konstantopedos P, et al. The effects of graded levels of calorie restriction: III. Impact of short term calorie and protein restriction on mean daily body temperature and torpor use in the C57BL/6 mouse. *Oncotarget*. 2015;6:18314–18337. doi:10.18632/oncotarget.4506
36. Mitchell SE, Delville C, Konstantopedos P, et al. The effects of graded levels of calorie restriction: II. Impact of short term calorie and protein restriction on circulating hormone levels, glucose homeostasis and oxidative stress in male C57BL/6 mice. *Oncotarget*. 2015;6(27):23213–23237. doi:10.18632/oncotarget.4003
37. Terao A, Steininger TL, Morairty SR, Kilduff TS. Age-related changes in histamine receptor mRNA levels in the mouse brain. *Neurosci Lett*. 2004;355:81–84. doi:10.1016/j.neulet.2003.10.061
38. Li B, Zhu JN, Wang JJ. Histaminergic afferent system in the cerebellum: structure and function. *Cerebellum Ataxias*. 2014;1:5. doi:10.1186/2053-8871-1-5
39. Ericson H, Watanabe T, Köhler C. Morphological analysis of the tuberomammmillary nucleus in the rat brain: delineation of subgroups with antibody again L-histidine decarboxylase as a marker. *J Comp Neurol*. 1987;263(1):1–24. doi:10.1002/CNE.902630102
40. Haas HL, Sergeeva OA, Selbach O. Histamine in the nervous system. *Physiol Rev*. 2008;88:1183–1241. doi:10.1152/physrev.00043.2007
41. Enwonwu CO, Worthington BS. Elevation of brain histamine content in protein-deficient rats. *J Neurochem*. 1975;24:941–945. doi:10.1111/j.1471-4159.1975.tb03659.x
42. Xu C, Michelsen KA, Wu M, Morozova E, Panula P, Alreja M. Histamine innervation and activation of septohippocampal GABAergic neurones: involvement of local ACh release. *J Physiol*. 2004;561(Pt 3):657–670. doi:10.1113/jphysiol.2004.071712
43. Kohen R, Yamamoto Y, Cundy KC, Ames BN. Antioxidant activity of carnosine, homocarnosine, and anserine present in muscle and brain. *Proc Natl Acad Sci U S A*. 1988;85:3175–3179. doi:10.1073/pnas.85.9.3175
44. He Y-C, Wu G-Y, Li D, et al. Histamine promotes rat motor performances by activation of H2 receptors in the cerebellar fastigial nucleus. *Behav Brain Res*. 2012;228(1):44–52. doi:10.1016/j.bbr.2011.11.029
45. Liu YC, Li F, Handler J, et al. Global regulation of nucleotide biosynthetic genes by c-Myc. *PLoS One*. 2008;3:e2722. doi:10.1371/journal.pone.0002722
46. Lane AN, Fan TW. Regulation of mammalian nucleotide metabolism and biosynthesis. *Nucleic Acids Res*. 2015;43:2466–2485. doi:10.1093/nar/gkv047
47. Weraarchakul N, Strong R, Wood WG, Richardson A. The effect of aging and dietary restriction on DNA repair. *Exp Cell Res*. 1989;181:197–204. doi:10.1016/0014-4827(89)90193-6
48. Lipman JM, Turturro A, Hart RW. The influence of dietary restriction on DNA repair in rodents: a preliminary study. *Mech Ageing Dev*. 1989;48:135–143. doi:10.1016/0047-6374(89)90045-6
49. Prapurna DR, Rao KS. Long-term effects of caloric restriction initiated at different ages on DNA polymerases in rat brain. *Mech Ageing Dev*. 1996;92(2–3):133–142. doi:10.1016/S0047-6374(96)01815-5
50. Kudo Y, Iwashita M, Iguchi T, Takeda Y. The regulation of L-proline transport by insulin-like growth factor-I in human osteoblast-like SaOS-2 cells. *Pflugers Arch*. 1996;432:419–425. doi:10.1007/s004240050153
51. Sharma S, Black SM. Carnitine homeostasis, mitochondrial function, and cardiovascular disease. *Drug Discov Today Dis Mech*. 2009;6(1–4):e31–e39. doi:10.1016/j.ddmec.2009.02.001
52. Green CL, Mitchell SE, Derous D, et al. The effects of graded levels of calorie restriction: IX. Global metabolomic screen reveals modulation of carnitines, sphingolipids and bile acids in the liver of C57BL/6 mice. *Aging Cell*. 2017;16:529–540. doi:10.1111/acel.12570
53. Green CL, Soltow QA, Mitchell SE, et al. The effects of graded levels of calorie restriction: XIII. Global metabolomics screen reveals graded changes in circulating amino acids, vitamins, and bile acids in the plasma of C57BL/6 Mice. *J Gerontol A Biol Sci Med Sci*. 2018;74(1):16–26. doi:10.1093/gerona/gly058
54. Lee CK, Weindruch R, Prolla TA. Gene-expression profile of the ageing brain in mice. *Nat Genet*. 2000;25:294–297. doi:10.1038/77046

55. Lu T, Pan Y, Kao S-Y, et al. Gene regulation and DNA damage in the ageing human brain. *Nature*. 2004;429(6994):883–891. doi:10.1038/nature02661
56. Arslan-Ergul A, Ozdemir AT, Adams MM. Aging, neurogenesis, and caloric restriction in different model organisms. *Aging Dis*. 2013;4:221–232.
57. Sohal RS, Ku H-H, Agarwal S, Forster MJ, Lal H. Oxidative damage, mitochondrial oxidant generation and antioxidant defenses during aging and in response to food restriction in the mouse. *Mech Ageing Dev*. 1994;74(1–2):121–133. doi:10.1016/0047-6374(94)90104-X
58. Youngman LD, Park JY, Ames BN. Protein oxidation associated with aging is reduced by dietary restriction of protein or calories. *Proc Natl Acad Sci U S A*. 1992;89:9112–9116. doi:10.1073/pnas.89.19.9112
59. Forster MJ, Dubey A, Dawson KM, Stutts WA, Lal H, Sohal RS. Age-related losses of cognitive function and motor skills in mice are associated with oxidative protein damage in the brain. *Proc Natl Acad Sci U S A*. 1996;93:4765–4769. doi:10.1073/pnas.93.10.4765
60. Quéméneur L, Gerland LM, Flacher M, Ffrench M, Revillard JP, Genestier L. Differential control of cell cycle, proliferation, and survival of primary T lymphocytes by purine and pyrimidine nucleotides. *J Immunol*. 2003;170:4986–4995. doi:10.4049/jimmunol.170.10.4986
61. Domínguez-López S, Howell RD, López-Canúl MG, Leyton M, Gobbi G. Electrophysiological characterization of dopamine neuronal activity in the ventral tegmental area across the light-dark cycle. *Synapse*. 2014;68:454–467. doi:10.1002/syn.21757
62. Shamsi NA, Salkeld MD, Rattanatray L, et al. Metabolic consequences of timed feeding in mice. *Physiol Behav*. 2014;128:188–201. doi:10.1016/j.physbeh.2014.02.021
63. Zhao Y, Zhao B. Oxidative stress and the pathogenesis of Alzheimer's disease. *Oxid Med Cell Longev*. 2013;2013:316523. doi:10.1155/2013/316523
64. Hwang O. Role of oxidative stress in Parkinson's disease. *Exp Neurobiol*. 2013;22:11–17. doi:10.5607/en.2013.22.1.11
65. Gil-Mohapel J, Brocardo PS, Christie BR. The role of oxidative stress in Huntington's disease: are antioxidants good therapeutic candidates? *Curr Drug Targets*. 2014;15:454–468. doi:10.2174/1389450115666140115113734